Substrate-Assisted Movement of the Catalytic Lys 215 during Domain Closure: Site-Directed Mutagenesis Studies of Human 3-Phosphoglycerate Kinase†

Beáta Flachner,‡ Andrea Varga,‡ Judit Szabó, László Barna, István Hajdú, Gergely Gyimesi, Péter Závodszky, and Mária Vas*

Institute of Enzymology, Biological Research Center, Hungarian Academy of Sciences, H-1518 Budapest, P.O. Box 7, Hungary

Received August 26, 2005; Revised Manuscript Received October 20, 2005

ABSTRACT: 3-Phosphoglycerate kinase (PGK) is a two-domain hinge-bending enzyme. It is still unclear how the geometry of the active site is formed during domain closure and how the catalytic residues are brought into the optimal position for the reaction. Comparison of the three-dimensional structures in various open and closed conformations suggests a large (10 Å) movement of Lys 215 during domain closure. This change would be required for direct participation of this side chain in both the catalyzed phospho transfer and the special anion-caused activation. To test the multiple roles of Lys 215, two mutants (K215A and K215R) were constructed from human PGK and characterized in enzyme kinetic and substrate binding studies. For comparison, mutants (R38A and R38K) of the known essential residue, Arg 38, were also produced. Drastic decreases (1500- and 500-fold, respectively), as in the case of R38A, were observed in the k_{cat} values of mutants K215A and K215R, approving the essential catalytic role of Lys 215. In contrast, the R38K mutation caused an only 1.5-fold decrease in activity. This emphasizes the importance of a very precise positioning of Lys 215 in the active site, in addition to its positive charge. The side chain of Lys 215 is also responsible for the substrate and anion-dependent activation, since these properties are abolished upon mutation. Among the kinetic constants mainly the K_m values of MgATP and 1,3-BPG are increased (∼20- and ∼8-fold, respectively) in the case of the neutral K215A mutant, evidence of the interaction of Lys 215 with the transferring phospho group in the functioning complex. Weakening of MgATP binding (a moderate increase in K_d), but not of MgADP binding, upon mutation indicates an initial weak interaction of Lys 215 with the γ-phosphate already in the nonfunctioning open conformation. Thus, during domain closure, Lys 215 possibly moves together with the transferring phosphate; meanwhile, this group is being positioned properly for catalysis.

PGK[1] catalyzes the reversible transfer of a phospho group from 1,3-bisphosphoglycerate (1,3-BPG) to ADP, yielding 3-phosphoglycerate (3-PG) and ATP during glycolysis. In addition, PGK was reported to influence DNA replication and repair in mammalian cell nuclei (*1*, *2*) and to stimulate viral mRNA synthesis in cytosol (*3*), and it may supply ATP for the Na^{2+} and Ca^{2+} ion pump (*4*, *5*). PGK also catalyzes phosphorylation of L-nucleoside analogues which are promising candidates for the inhibition of viral replication and treatment of cancer (*6*−*8*). Thereby, PGK regulates the level of pharmacologically active triphosphate forms of these compounds in the cell (*9*). Independent of the kinase activity, extracellular PGK was recently shown to have a thiol reductase activity on plasmin as a substrate, leading to formation of angiostatine fragments (*10*−*13*), which inhibits angiogenesis of tumor cells (*14*, *15*).

PGK is a typical two-domain hinge-bending enzyme (*16*), with a highly conserved structure (*17*, *18*). The N-terminal domain has a basic patch region for binding of 3-PG (*19*−*27*), and the C-terminal domain contains the binding site for the nucleotide substrates, MgADP and MgATP (*20*−*23*, *27*−*34*), as revealed by both crystallographic (*19*−*24*, *28*−*30*) and NMR chemical shift perturbation (*25*, *27*, *31*−*34*) as well as relaxation (*25*, *27*, *31*−*34*) studies. No such definitive information is available for the interaction with the highly unstable 1,3-BPG. For the catalyzed phospho transfer, the two domains must close together, as evidenced by crystallographic (*21*, *22*) and diffuse-X-ray scattering (*35*−*37*) studies. The spectacular difference between the open (black) and closed (red) conformations is illustrated by their superposition (Figure 1A).

3-PG is bound nearly in the same way in all PGK crystal structures. In agreement, site-directed mutagenesis studies (*24*−*26*, *38*−*43*) have confirmed the importance of the basic residues at the inner surface of the N-domain in binding of

† Supported by OTKA Grants D 048578, T 043446, and T 046412 from the Hungarian National Research Foundation.

* To whom correspondence should be addressed: Institute of Enzymology, BRC, Hungarian Academy of Sciences, H-1518 Budapest, P.O. Box 7, Hungary. Telephone: 36 1 279 3152. Fax: 36 1 466 5465. E-mail: vas@enzim.hu.

‡ These authors contributed equally to this work.

[1] Abbreviations: PGK, 3-phospho-D-glycerate kinase or 3-phospho-D-glycerate 1-phosphotransferase (EC 2.7.2.3); hPGK, human PGK; GAPDH, D-glyceraldehyde-3-phosphate dehydrogenase (EC 1.2.1.12); HK, hexokinase (EC 2.7.1.1); G6PDH, glucose-6-phosphate 1-dehydrogenase (EC 1.1.1.49); CM, carboxymethyl; 3-PG, 3-phospho-D-glycerate; 1,3-BPG, 1,3-bisphosphoglycerate; AMP-PNP, β,γ-imidoadenosine 5′-triphosphate; AMP-PCP, β,γ-methyleneadenosine 5′-triphosphate; DSC, differential scanning microcalorimetry; IPTG, isopropyl β-D-thiogalactopyranoside; CD, circular dichroism; Nbs_2, Ellmann's reagent, 5,5′-dithiobis(2-nitrobenzoic acid).

10.1021/bi051726g CCC: $30.25
Published on Web 12/01/2005

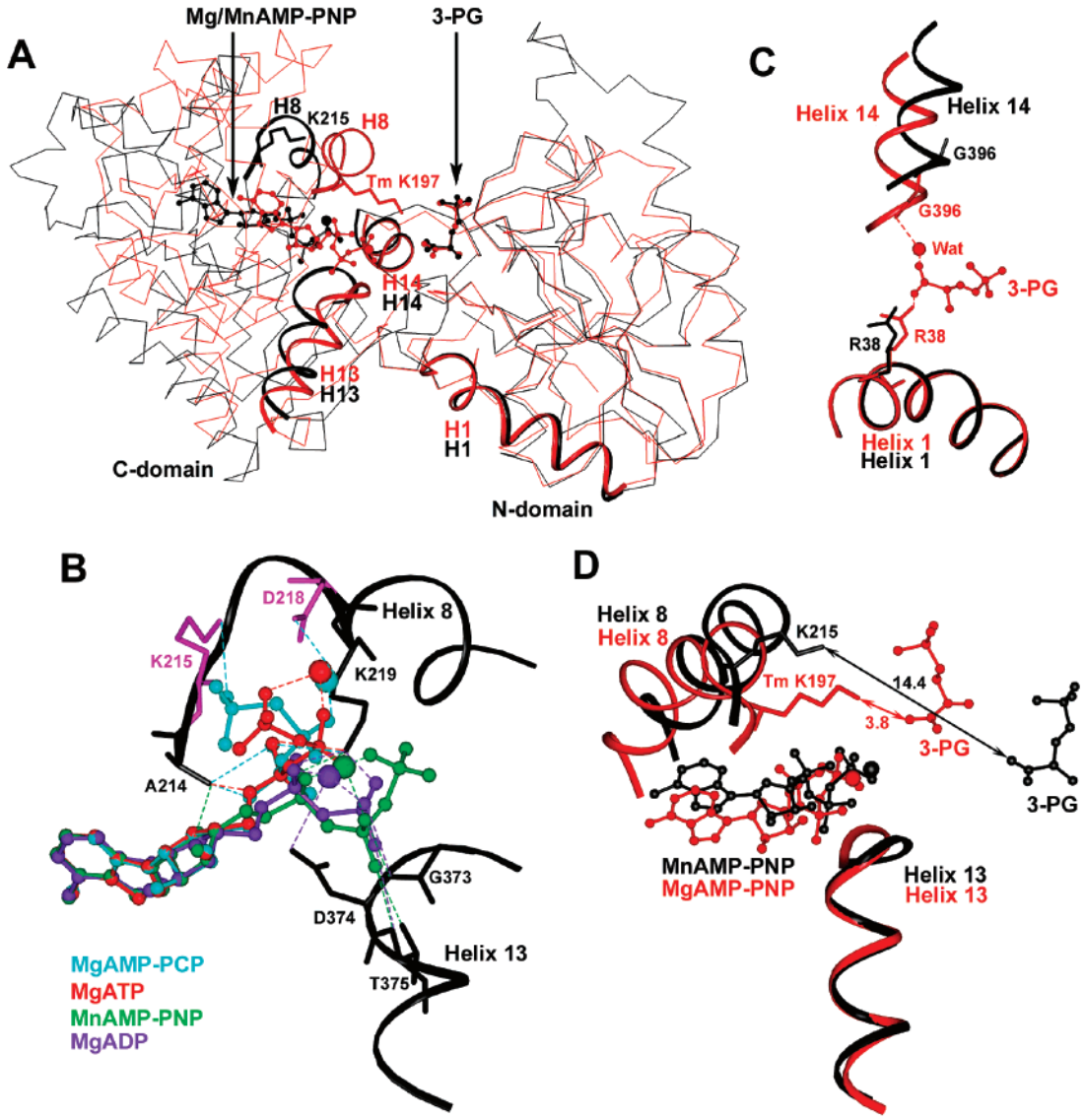

FIGURE 1: Superposition of the open and closed PGK conformations (A, C, and D) and the various binding modes of the nucleotides (B). In panel A, the traces (Cα) of the open (black) and closed (red) conformations of pig muscle (*20*) and *Th. maritima* (*22*) PGKs, respectively, were superimposed according to the backbone atoms of the core β-strands of the N-terminal domain. In panel B, the separate crystal structures of MgADP (purple) as bound to *B. stearothermophilus* PGK (*28*), MgAMP-PCP (cyan) as bound to pig muscle PGK (*29*), and MgATP (red) as bound to pig muscle PGK (*30*) are superimposed according to the adenine and ribose rings onto MnAMP-PNP (green) as bound to pig muscle PGK (*20*). Residues Lys 215 and 218 are highlighted in violet. The dashed lines represent H-bonds (up to 3.5 Å) and ionic interactions (up to 4.0 Å). In panel C, the open (black) and slightly closed (red) structures of substrate-free pig muscle (Z. Kovári, G. Náray, and M. Vas, unpublished observations) and the 3-PG binary complex of the pig muscle (*19*) PGKs, respectively, were superimposed according to helix 1. In panel D, the open (black) and closed (red) conformations of pig muscle (*20*) and *Th. maritima* (*22*) PGKs, respectively, were superimposed according to helix 13. In all cases, helices 1, 8, 13, and 14 are highlighted as ribbons and the bound 3-PG and the ATP analogue Mg/MnAMP-PNP are shown as ball-and-stick models. The distances indicated by arrows are given in angstroms.

this substrate. The extended basic patch can also bind various anions, as shown by various techniques (*42*, *44*−*47*). Anions not only inhibit the enzyme by replacing the substrate but also can increase the enzyme activity at low concentrations (*48*−*50*), which is similar to activation by the excess of substrates (*49*, *51*, *52*). These activation phenomena are peculiar regulatory behaviors of PGK, the molecular basis of which is still not completely understood. The anion activation is diminished or completely abolished in the case of some basic patch mutants (*39*, *41*, *43*), but the data have not yet provided a satisfactory explanation about the location of the activating site and the molecular mechanism of activation. A hypothesis was put forward about formation of the activating anionic site only upon domain closure (*50*). Accordingly, in the catalytically competent closed conformation, the constituent basic residues of this site originate from both domains, including part of the basic patch of the N-domain and Lys 215 (mammalian PGK sequence numbering) of the C-domain.

In contrast to that of 3-PG, the binding mode of the nucleotide substrates is not a unique type. Adenine and ribose rings bind similarly in all structures (*20*−*23*, *28*−*30*), but the position and interaction of the phosphate chains are different. The phosphates of MgADP (*21*, *28*) or Mg/MnAMP-PNP (*20*, *22*), an unreactive analogue of ATP, bind to the N-terminus of helix 13, but the γ-phosphate of another ATP analogue, MgAMP-PCP, is bound rather close to the N-terminus of helix 8 (*29*). The positions of these helices

(among the other important ones) in the active site region of PGK molecule are indicated in Figure 1A. Phosphates of MgATP occupy an intermediate position between these two states, as shown by the recently published MgATP binary complex structure (*30*). Variations of the binding mode of the nucleotides are illustrated in Figure 1B. On this basis, we assumed fluctuation of the flexible MgATP phosphates between the N-termini of helices 8 and 13. Thus, besides the previously identified nucleotide site at the end of helix 13, according to our hypothesis, an alternative site should also exist close to helix 8 for the phosphate chain of the nucleotides. The side chains of the completely conserved Lys 215 and the largely conserved Asp 218 (colored violet in Figure 1B) of helix 8 may be the constituents of this site. On the other hand, from the closed structure of the MgAMP-PNP−3-PG ternary complex of *Thermotoga maritima* (red structure in panels A and D of Figure 1), Lys Tm197[2] (equivalent to Lys 215 in the sequence of the mammalian PGK) was hypothesized to participate in stabilization of the transferring phospho group during catalysis (*22*) together with the previously identified essential catalytic residue, Arg 38/Tm36 (*39*, *41*), which is located in helix 1 of the N-domain (Figure 1C). In the open structures of pig muscle PGK (black structure in panels A, B, and D of Figure 1), however, the side chain of Lys 215 is situated outside of the active site and has proven to be very mobile (*20*, *29*, *30*). Taken together, surveying the three-dimensional (3D) structure of PGK in various open and closed conformations revealed that the residue Lys 215/Tm197 moves more than 10 Å during domain closure (Figure 1A,D), and this movement may be aided by its occasional interaction with the nucleotide. This large movement would be consistent with the assumed roles of Lys 215 both in stabilization of the transferring phospho group and in formation of the activating anion site, proposed from previous modeling studies (*50*).

To test the multiple roles of Lys 215 (mammalian PGK numbering) in this work, we have carried out site-directed mutagenesis studies on hPGK. Although no 3D structure of hPGK has been determined, its primary sequence is identical (up to 98%) to that of pig muscle PGK, for which various crystal structures (*24*−*26*, *38*−*43*) are known. Thus, Lys 215 was replaced with either the neutral Ala or the similarly charged Arg, and the mutants (K215A and K215R) were characterized in enzyme kinetic and substrate binding studies. For comparison, mutants (R38A and R38K) of Arg 38, the known essential residue, were also expressed and investigated. Besides, the possible participation of Asp 218 in interaction with the ATP phosphates (through Mg^{2+}) was also assessed by replacing it with its neutral counterpart, Asn, in the mutant D218N.

MATERIALS AND METHODS

Chemicals. Na salts of 3-PG, ATP, and ADP were from Boehringer. The substrates MgATP and MgADP were formed by addition of $MgCl_2$ (Sigma) to ATP and ADP, respectively. The dissociation constants of MgATP and MgADP were taken to be 0.1 and 0.6 mM, respectively, obtained by averaging the data in the literature (*53*−*57*). NADH, NADP, and glucose were from Sigma. 1,3-BPG was prepared from glyceraldehyde 3-phosphate (Sigma) according to the Negelein method (*58*) with the modifications described by Furfine et al. (*59*). IPTG (Fermentas), chloramphenicol, and ampicillin (Sigma) were used for the fermentation. The QuikChange mutagenesis kit was purchased from Stratagene. Primers were produced in Biological Research Center (Hungarian Academy of Sciences, Szeged, Hungary). All other chemicals were reagent grade commercial preparations.

Enzymes. The hPGK (*52*) gene cloned in the pET11c vector was a gift from P. J. Hogg (University of New South Wales, Sydney, Australia). The enzyme was overexpressed in the *Escherichia coli* BL21-CodonPlus (DE3)-RIL (Stratagene) strain, extracted by sonication, and purified by double-ammonium sulfate fractionation and CM-Sepharose chromatography, based on the method described for purification of pig muscle PGK (*19*). For the experiments, the eluted protein was dialyzed against 20 mM Tris-HCl buffer (pH 7.5) containing 1 mM dithiothreitol and stored in a frozen state at −80 °C at ∼0.4 mM (∼20 mg/mL). Under these conditions, PGK did not loose its activity for several months.

GAPDH was prepared from pig muscle and stored as a microcrystal suspension in ammonium sulfate (*60*). HK and G6PDH, in the form of ammonium sulfate precipitates, were from Sigma. G6PDH was purified on a Superose12 column (Pharmacia) to clear it from the contaminant PGK. Crystals of these auxiliary enzymes were dialyzed against 20 mM Tris-HCl buffer (pH 7.5) containing 1 mM dithiothreitol, to remove $(NH_4)_2SO_4$.

Site-Directed Mutagenesis. Residues 38, 215, and 218 of hPGK were mutated with the QuikChange site-directed mutagenesis kit from Stratagene following the instructions of the manufacturer. The following primers were used: 5′-CAAACAACCAGGCGATTAAGGCTGCTGTCC-3′ and 5′-GGACAGCAGCCTTAATCGCCTGGTTGTTTG-3′ for the R38A mutant, 5′-GATAACAAACAACCAGAAGATTAAGGCTGCTGTCC-3′ and 5′-GGACAGCAGCCTTAATCTTCTGGTTGTTTGTTATC-3′ for the R38K mutant, 5′-CATCCTGGGCGGAGCTGCAGTTGCAGACAAGATC-3′ and 5′-GATCTTGTCTGCAACTGCAGCTCCGCCCAGGATG-3′ for the K215A mutant, 5′-CTGGGCGGAGCTAGAGTTGCAGACAAGATCC-3′ and 5′-GGATCTTGTCTGCAACTCTAGCTCCGCCCAG-3′ for the K215R mutant, and 5′-GGCGGAGCTAAAGTTGCAAACAAGATCCAGCTC-3′ and 5′-GAGCTGGATCTTGTTTGCAACTTTAGCTCCGCC-3′ for the D218N mutant. The mutations were checked by DNA sequencing.

Enzyme Kinetic Studies. The activity of hPGK was measured in both directions of the enzyme reaction. With the substrates 3-PG and MgATP, the reaction was followed spectrophotometrically at 340 nm, when NADH reduced 1,3-BPG, the product of the PGK-catalyzed reaction, in the presence of GAPDH (*61*). The substrate saturation curves were fitted using the following equation elaborated by Szilágyi and Vas (*50*) for the case of activation by the excess of substrates:

$$v = v_S \frac{[S]}{K_{cat}^S + [S]} + v_S(a-1)\frac{[S]}{K_{cat}^S + [S]}\frac{[S]}{K_{act}^S + [S]} \quad (1)$$

The first term represents a simple hyperbolic saturation of

[2] The numbering of residues throughout the text refers to the human PGK sequence unless quoted differently, e.g., Tm (*Thermotoga maritima*), Tb (*Trypanosoma brucei*), and Bs (*Bacillus stearothermophilus*).

the catalytic site with the substrate (S), if the activation by the excess substrate were not taking place. Thus, v_S stands for the hypothetical activity at saturation of the catalytic site by the substrate. The second term represents saturation of the activating site, which is a nonhyperbolic function. In accordance with the fast equilibration of binding of substrate to PGK, K^S_{cat} and K^S_{act} are the dissociation constants for the catalytic and activating sites, respectively. The coefficient a (≥ 1) is the factor by which activity increased when the substrate bound to the activating site.

Anion activation and inhibition studies were carried out in the presence of pyrophosphate, since it was found to be the most effective multivalent anion, as compared to sulfate, phosphate, and citrate (*49*; A. Varga and M. Vas, unpublished observations). To avoid usage of the large excess of chloride ion, only a limited amount of $MgCl_2$ was added to the reaction mixture to ensure complexation with ATP. In these experiments, GAPDH, the coupling enzyme, was used at a concentration sufficiently high to counterbalance its inhibition by pyrophosphate. To describe the simultaneous activating and inhibiting effects caused by anions, the following formula is used:

$$v = v_0 + v_0(a-1)\frac{[A]}{K^A_{act} + [A]} - \left[v_0 + v_0(a-1)\frac{[A]}{K^A_{act} + [A]}\right]\frac{[A]^n}{K^A_{inh} + [A]^n} \quad (2)$$

where v_0 stands for the activity of the enzyme in the absence of bound anion (A) at fixed substrate concentrations and a (≥ 1) is the factor by which activity is increased. K^A_{act} and K^A_{inh} are the apparent dissociation constants for the sites of activation and inhibition by anion (A), respectively. The real constants for the investigated anion are related to these apparent constants according to the following equations, which assume competitive replacement of anions by the substrates, both in the activating and at the catalytic sites, and take into account the substrate concentrations applied in the experiment:

$$K^A_{act} = \frac{K^A_{act,app}K^S_{act}}{[S] + K^S_{act}} \quad (3)$$

$$K^A_{inh} = \frac{K^A_{inh,app}K^S_{cat}}{[S] + K^S_{cat}} \quad (4)$$

Equation 2 is a modified form of one published previously by Szilágyi and Vas (*50*) and assumes the existence of n interacting sites for the inhibiting anions, instead of one. Here all inhibiting sites are characterized by a single average dissociation constant.

The activity measurements with the substrates 1,3-BPG and MgADP were followed by reduction of NADP either spectrophotometrically at 340 nm or fluorimetrically (excitation at 355 nm and emission at 455 nm), when the product MgATP phosphorylates glucose by HK and the generated hexose 6-phosphate reduces NADP, in the presence of G6PDH. The substrate saturation curves, within the investigated range of substrate concentrations, could be satisfactorily fitted by the simple Michaelis−Menten equation. Due to the extremely low K_m value of 1,3-BPG, its direct determination has met with difficulty even in case of the more sensitive fluorimetric detection of NADH. Namely, at concentrations of 1,3-BPG equal to or lower than its K_m value, the total observed spectroscopic change would be too low for accurate rate determinations. Therefore, we took advantage of the competitive displacement of 1,3-BPG by 3-PG, i.e., determined the apparent K_m value of 1,3-BPG in the presence of various, at each case constant, concentrations of the inhibitor, 3-PG. From the data, the real K_m value could be calculated on the following basis:

$$K_m = \frac{K^{app}_m K_I}{[I] + K_I} \quad (5)$$

where I and K_I represent 3-PG and its competitive inhibitory constant with respect to 1,3-BPG, respectively. The K_I value was taken to be equal to the K_m of 3-PG.

All the kinetic experiments were carried out at 20 °C in 20 mM Tris-HCl buffer (pH 7.5) containing 1 mM dithiothreitol. This buffer ensured the low ionic strength required for studies of the effect of low concentrations of anions.

Substrate Binding Studies. The dissociation constants (K_d) of binding of various substrates or anions to PGK were determined on the basis of their protective effects against modification of the enzyme reactive thiols. Pig and horse muscle PGK molecules have two similarly reactive thiol groups in addition to the five slowly reacting buried thiols. The rate of modification of the reactive thiols is specifically decreased by each of the bound substrates (*62*, *63*). We show here that hPGK and its present mutants (except R38A) behave similarly. The R38A mutant exhibits a different thiol reactivity pattern: besides the two fast-reacting thiols, its molecule has three additional reactive thiol groups with intermediate reactivity and only two slowly reacting ones (Figure 4B). The reactivity of the latter ones is comparable with that of the five buried thiols of the wild-type enzyme. In all cases, however, the rate of modification of the two fast-reacting thiols with Nbs_2 was sensitively decreased upon substrate binding. Thus, for all PGK forms, the rate of this modification was measured as a function of substrate concentration and analyzed as described previously for the K_d determinations (*29*). Under these conditions, the extremely strong binding of 1,3-BPG did not allow the direct determination of its K_d. Its apparent value could, however, be determined in the presence of a high concentration of 3-PG, i.e., by taking advantage of its competitive displacement by this other substrate. By knowing the separately determined K_d of 3-PG, we determined the real K_d of 1,3-BPG by using the formula

$$K_d = \frac{K^{app}_d K_L}{[L] + K_L} \quad (6)$$

where L and K_L represent 3-PG and its dissociation constant, respectively.

DSC Experiments. The DSC measurements were performed in a MicroCal VP-DSC-type microcalorimeter (MicroCal Inc.) with a cell volume of 0.51 mL, at a constant scan rate of 60 °C/h. The protein concentration was 0.13

Table 1: Summary of the Functional Properties of the Wild-Type and Mutant PGKs[a]

constant	hPGK	K215A	K215R	D218N	R38A	R38K	R38K/K215R
kinetic							
reverse direction							
k_{cat} ($v_S a$)	50000 ± 3000	29 ± 3	105 ± 9	16000 ± 1000	27 ± 2	33000 ± 2500	10 ± 2
a	3.8 ± 0.6	1	1	1.7 ± 0.5	1	3.9 ± 0.7	1
K_{cat}^{MgATP} or K_m^{MgATP}	0.11 ± 0.03	2.47 ± 0.2	0.57 ± 0.03	0.15 ± 0.04	0.96 ± 0.07	0.08 ± 0.02	0.43 ± 0.03
K_{cat}^{3-PG} or K_m^{3-PG}	0.10 ± 0.02[b] 0.05 ± 0.01[c]	0.41 ± 0.04	0.35 ± 0.02	0.42 ± 0.20	4.5 ± 0.4	0.28 ± 0.01	0.76 ± 0.06
$K_I^{pyrophosphate}$	0.22 ± 0.07	0.51 ± 0.15	0.53 ± 0.21	0.51 ± 0.05	0.13 ± 0.09	0.35 ± 0.10	0.49 ± 0.12
forward direction							
k_{cat} (V_{max})	158000 ± 25000	47 ± 5	291 ± 10	nd[d]	360 ± 20	nd[d]	nd[c]
K_m^{MgADP}	0.12 ± 0.02	0.15 ± 0.03	0.11 ± 0.03	nd[d]	0.10 ± 0.03	nd[d]	nd[c]
$K_m^{1,3-BPG}$	0.0005 ± 0.0002	0.0038 ± 0.0003	0.0014 ± 0.0002	nd[d]	0.29 ± 0.01	nd[d]	nd[c]
binding							
K_d^{MgATP}	0.33 ± 0.15	1.45 ± 0.15	0.83 ± 0.18	0.30 ± 0.15	0.59 ± 0.20	0.46 ± 0.10	0.79 ± 0.13
K_d^{MgADP}	0.029 ± 0.004	0.045 ± 0.007	0.024 ± 0.007	nd[d]	0.035 ± 0.009	0.022 ± 0.001	0.023 ± 0.002
K_d^{3-PG}	0.035 ± 0.008	0.039 ± 0.01	0.037 ± 0.004	0.042 ± 0.004	0.94 ± 0.30	0.11 ± 0.01	0.14 ± 0.05
$K_d^{1,3-BPG}$	0.000056 ± 0.000024	0.000052 ± 0.000019	0.000047 ± 0.000015	nd[d]	0.009± 0.002	nd[d]	0.000052 ± 0.000020
$K_d^{pyrophosphate}$	0.21 ± 0.04	0.28 ± 0.05	0.20 ± 0.05	nd[d]	nd[d]	nd[d]	nd[c]

[a] Rate (inverse minutes) and equilibrium (millimolar) constants are determined from the type of experiments shown in Figures 2, 3, and 4B. $K_{act,app}^{S}$ values (not listed) could be determined only with a relatively large error and varied between 10 and 30 mM in all cases where $a \neq 1$. [b] In the presence of 10 mM MgATP. [c] In the presence of 2.5 mM MgATP. [d] Not determined.

mg/mL (0.003 mM) in all experiments. All samples were carefully degassed before the experiments. The data were analyzed using MicroCal Origin 5.0. The melting temperature (T_m) was determined after subtraction of the instrumental baseline.

CD Spectroscopy. The measurements were performed in a JASCO 720 spectropolarimeter in both far-UV (200−260 nm) and near-UV (260−350) regions. The experiments were carried out at 20 °C using 0.1 and 1 cm path length cells, respectively, and the protein concentrations were 0.4 and 2.5 mg/mL (i.e., 0.009 and 0.056 mM), respectively.

Modeling of Binding of a Ligand to PGK. Docking of 1,3-BPG and phosphate ion into a PGK molecule has been carried out by using GOLD version 2.2 (*64*). The X-ray structure of PGK from *Trypanosoma brucei* (PDB entry 13PK) chain B was used as the target of the docking. The partial charge distribution of the 1,3-BPG and phosphate ion was calculated by MOPAC. Hydrogens were added to the protein and the ligands assuming the condition of pH 7.5. Ligands, but not the protein, were considered to be flexible. The site for all docking processes was defined to encompass all atoms within a 19 Å radius whose center was the Cα atom of Arg 65. Twenty individual docking cycles were carried out for each ligand with the following main parameters: pop size, 100; maxops, 200000; early_termination, off; score, gold. At first, for docking of 1,3-BPG, we removed every heteroatom except the ADP and the magnesium ion with its coordinating water molecules. Second, we merged the best-ranked 1,3-BPG structure into the initial structure and continued the docking with the phosphate ions with the same protocol. Alternatively, some of the water molecules coordinating magnesium ion were also removed before docking. The rms deviation of individual docking was within 5.74 and 0.1 Å for 1,3-BPG and phosphate ion, respectively. Alternatively, docking with other anions (pyrophosphate and citrate) or with the substrates (3-PG and 1,3-BPG) was carried out, instead of docking with phosphate.

The electrostatic potential map of the PGK ternary complex containing the bound MgADP and the best-docked 1,3-BPG was calculated by using Insight II (version 2000L, Biosym/MSI, San Diego, CA). The same software was used for visualizing and analyzing the molecular details of PGK structures.

RESULTS

Enzyme Kinetic Characterization of the K215A, K215R, and D218N Mutants of hPGK. Enzyme kinetic studies, carried out in both directions of the PGK-catalyzed reaction, revealed drastic decreases in the enzyme activities of the mutants K215A and K215R (1500- and 500-fold, respectively), as compared to that of wild-type hPGK, while the D218N mutation resulted in a decrease of only ∼3-fold. The activity values of all mutants are summarized in Table 1. Thus, either replacement of Lys 215 leads to an activity loss similar in magnitude to that found for the R38A mutant of yeast PGK (*41*) and of hPGK in this work. In contrast to the expectations, the R38K mutant has hardly lost its activity (only ∼1.5-fold) compared to wild-type hPGK.

Considering the relatively high activity of the mutant R38K prompted us to try to improve further the activity by preparing the double mutant R38K/K215R, i.e., to see whether the possible roles of Arg 38 and Lys 215 in stabilizing the transferring phospho group are interchangeable. The double mutant, however, in all aspects behaved very much like the largely inactive enzyme bearing only the single K215R mutation.

The saturation curves with the substrates 3-PG and MgATP (i.e., in the reverse direction of glycolysis) for wild-type hPGK can be described by the kinetic equation assuming activation by the excess substrate (Figure 2A,B). This behavior of the human enzyme is very similar to that of yeast (*49*, *51*, *52*) and pig muscle (*50*) PGKs. The experimental points can be fitted by the same equation and resulted in very similar kinetic constants as derived previously for pig muscle PGK (*50*). Both mutations of Lys 215 completely abolish this activation, and their substrate saturation curves follow a simple hyperbolic Michaelis−Menten relationship (Figure 2). This behavior of Lys 215 mutants is similar to

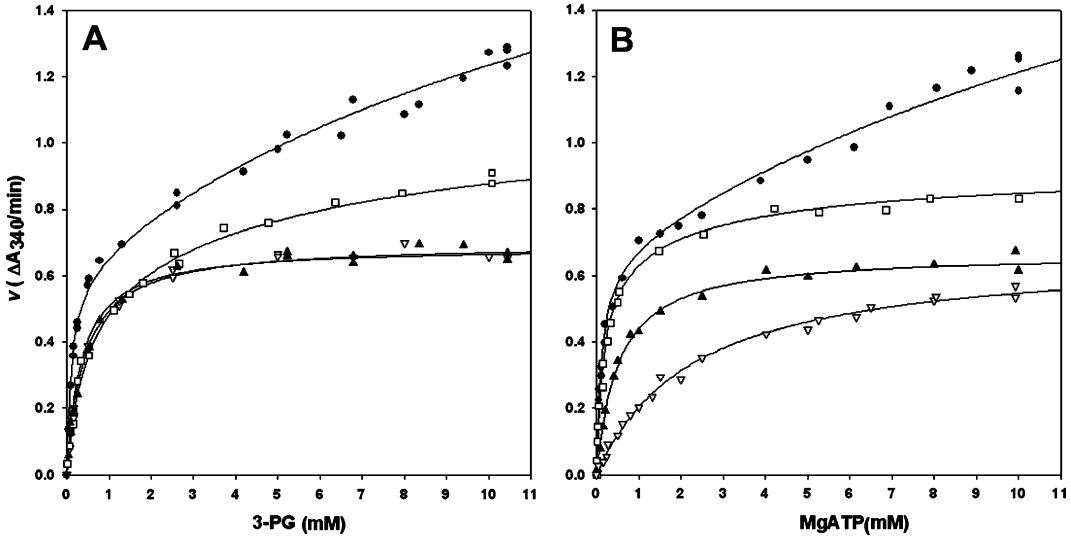

FIGURE 2: Comparison of the kinetics of wild-type and mutant PGKs. Activities of 8 nM wild-type (●), 22.8 nM D218N (□), 3.8 μM K215A (▽), and 0.9 μM K215R (▲) PGKs were measured in the presence of 10 mM MgATP (obtained from 10 mM ATP and 12.5 mM $MgCl_2$) as a function of 3-PG concentration (A) or in the presence of 10 mM 3-PG as a function of MgATP concentration (with a constant 12.5 mM $MgCl_2$) (B). Curve fitting was carried out by using eq 1 for the wild-type hPGK and the mutant D218N, and by using the Michaelis−Menten equation for K215A and K215R mutants.

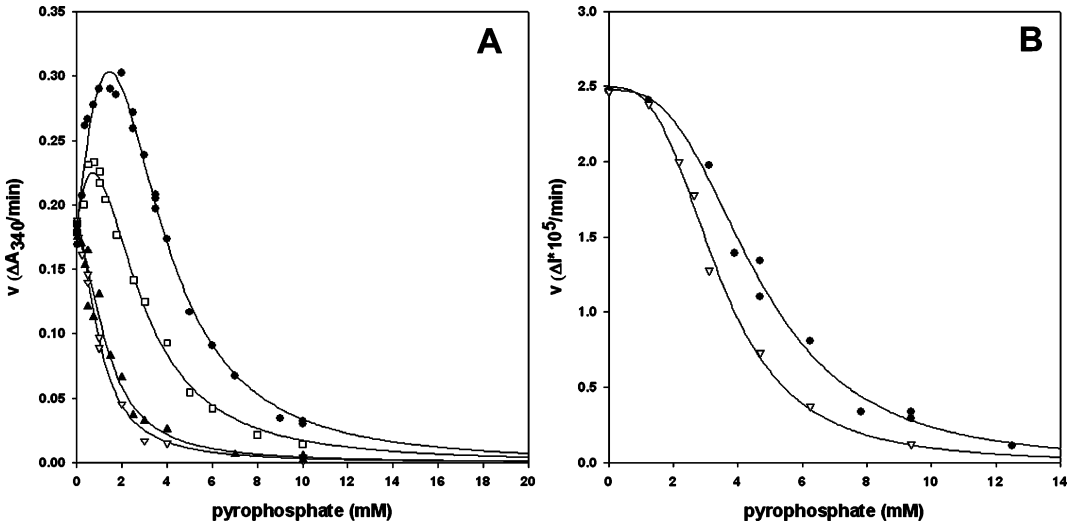

FIGURE 3: Activation and inhibition by pyrophosphate. Activities of 10.7 nM wild-type (●), 17.4 nM D218N (□), 4.15 μM K215A (▽), and 0.77 μM K215R (▲) PGKs were measured with the substrates 0.5 mM 3-PG and 0.5 mM MgATP (0.6 mM ATP and 1 mM $MgCl_2$) and as a function of the pyrophosphate concentration (A). Activities of 0.31 nM wild-type (●) and 1.12 μM K215A (▽) PGKs were also measured with the substrates 0.01 mM 1,3-BPG and 0.13 mM MgADP (0.145 mM ADP and 5 mM $MgCl_2$) and as a function of the pyrophosphate concentration (B). Activities were recorded spectrophotometrically (A) or fluorimetrically (B), as described in Materials and Methods. Curve fitting was carried out by using eq 2. With the substrate 1,3-BPG, $a = 1$ (i.e., no activation) was found to be valid for wild-type hPGK (B). In the cases of K215A and K215R mutants, $a = 1$ was applied, independent of the reaction direction (A and B). In all cases, an average of n values of 1.85 ± 0.2 was obtained.

that of the mutant R38A (not shown). The D218N mutation only largely reduces the level of activation by the excess substrate, and the active mutant (R38K) behaves like the wild-type enzyme. In the reaction starting from 1,3-BPG and MgADP (i.e., in the forward direction of glycolysis), the substrate saturation curves for either the wild-type hPGK or its investigated mutants apparently do not exhibit activation by the excess substrates and follow simple Michaelis−Menten-type kinetics (not shown). This finding is in agreement with previous data obtained with rat liver PGK (*65*), but it does not necessarily exclude the operation of an activation mechanism at higher concentrations of the substrates in this direction of the catalysis, as reported with human erythrocyte PGK (*52*).

The kinetic constants are summarized in Table 1. Except for the active mutant R38K, significant changes have been observed. The K_m of 3-PG is increased only moderately in cases of mutations of Lys 215 and Asp 218, while the largest increase (40-fold) was found in case of the mutant R38A. The latter finding is in agreement with the previous report on yeast PGK (*41*). The K_m of MgATP is also increased differently upon mutation. The largest change (~20-fold) is caused by mutation of Lys 215 into Ala (K215A), while mutation into Arg (K215R) caused only a smaller increase. Mutation of Arg 38 into Ala (R38A) also increased moderately the K_m of MgATP, in agreement with the finding with yeast PGK (*41*), while for the mutant D218N, no change could be detected in the corresponding K_{cat} value. The

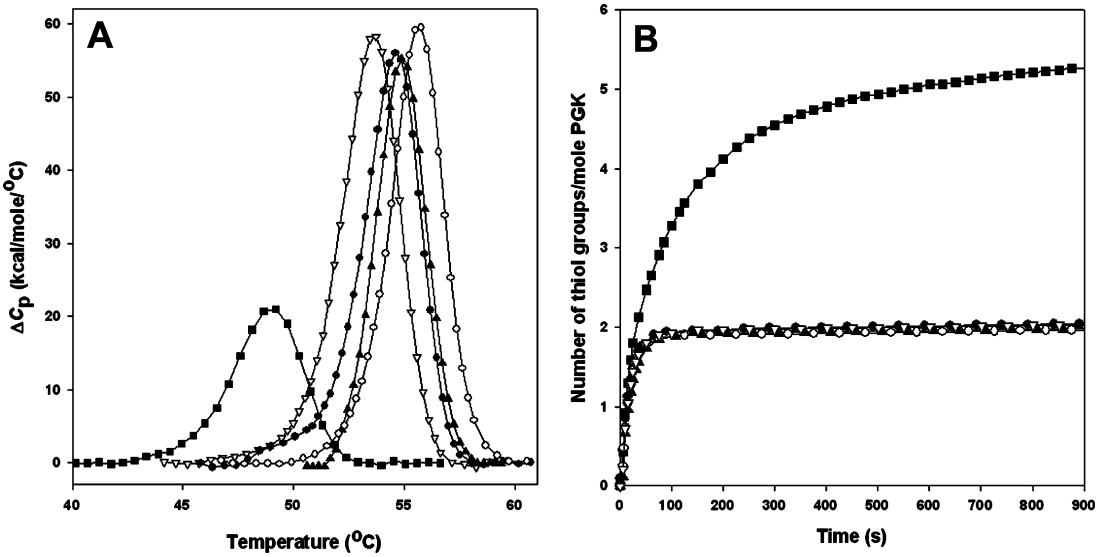

FIGURE 4: Effect of mutation on thermal stability and thiol reactivity of PGK. DSC heat transition curves (A) as well as the time courses of thiol reactivity (B) were determined with substrate-free wild-type (●), K215A (▽), K215R (▲), R38A (■), and R38K (○) PGKs. The T_m values, obtained from panel A, in the same order are 54.7, 53.6, 54.9, 49.0, and 55.7 °C, respectively. In panel B, the reaction of 0.009 mM PGK with 0.05 mM Nbs_2 was followed at 412 nm and the number of reacted thiol groups per mole PGK was calculated using an ϵ_{412} of 14 150 M^{-1} cm^{-1} (*81*).

increase in the K_m of 1,3-BPG follows the same order as for the K_m of MgATP. The largest increase (600-fold) of the K_m of 1,3-BPG was obtained for the mutant R38A. The K_m of MgADP is not changed upon mutation of either Lys 215 or Arg 38.

Effects of Mutations on Anion Activation and Inhibition. In the reaction with 3-PG and MgATP, wild-type hPGK exhibits activation and inhibition as a function of increasing concentrations of multivalent anions, such as pyrophosphate (Figure 3A). This peculiar behavior of PGK was observed long ago for the yeast enzyme (*48*, *49*, *66*), but was described quantitatively much later for the pig muscle enzyme (*50*). According to this model, two separate sites have been assumed for activating and inhibiting anions, but more importantly, these sites are exclusive characteristics of the active, domain-closed PGK conformation; i.e., they are formed (or completed) upon domain closure. Here with hPGK we have extended the previous measurements to other physiological anions (phosphate, citrate, and pyrophosphate) and various substrate concentrations (data not shown). Careful quantitative analysis of the data based on the published equation that assumes one activating and one inhibiting site (*50*), however, has always led to a significant deviation from the fitted curve. This observation prompted us to modify the model. To this end, the data were found to be best described by a model that assumes one activating and two cooperatively interacting inhibiting anionic sites (eq 2) and exemplified by using the most effectively interacting pyrophosphate in Figure 3A. This model is fully consistent with the structural observation of two separate phosphate sites (cf. Discussion).

As for the mutants produced here, mainly activation is affected, and the inhibition is much less changed. Both mutations of Lys 215 completely abolish anion activation [similar to the previous (*39*) and present findings (not shown) with the mutant R38A], but mutation of Asp 218 only largely reduces it (Figure 3A). Thus, mutations influence anion activation in a manner similar to that observed above for the activation by the excess substrate. In addition, almost all the investigated mutations cause a moderate increase in the K_I values (Table 1), i.e., lead to weakening of the interaction with the inhibiting anion. It may also be noted that the two interacting inhibitory sites could only be characterized by a single average K_I value, and competition of pyrophosphate against both substrates was equally assumed.

In the reaction with 1,3-BPG and MgADP, neither the wild-type hPGK nor its K215A mutant exhibits anion activation, only inhibition (Figure 3B). Moreover, the interaction with the inhibiting pyrophosphate is weakened upon mutation of Lys 215, similar to the above findings. The absence of activation is fully consistent with the simple Michaelis−Menten kinetic behavior and argues for the absence of the activation phenomena, even in case of the wild-type enzyme in this direction of the catalysis.

Binding of Substrate and Anion to K215A, K215R, and D218N Mutants of hPGK. To assess whether the increases in the substrate K_m values are reflected in their K_d values, binding studies were carried out. In general, no or much smaller changes have been observed in the K_d values upon mutation, as compared to the K_m values of the respective substrates. There were no detectable differences between Lys 215 mutants and wild-type hPGK in terms of the K_d values of MgADP, 3-PG, and 1,3-BPG. The K_d values of MgATP, however, increased significantly, although moderately, for both K215A and K215R (Table 1). In contrast, mutation of Arg 38 into Ala has led to large increases in the K_d values of both 3-PG and 1,3-BPG, while K_d values of the nucleotide substrates are not much affected. In cases of D218N and R38K mutants, no significant changes in K_d values of either of the substrates have been observed. Since anion activation experiments revealed the disappearance or significant decrease in the level of activation by pyrophosphate upon mutation, the K_d values of binding of pyrophosphate to the Lys 215 mutants were also determined. Among these values, however, no significant differences were found (Table 1).

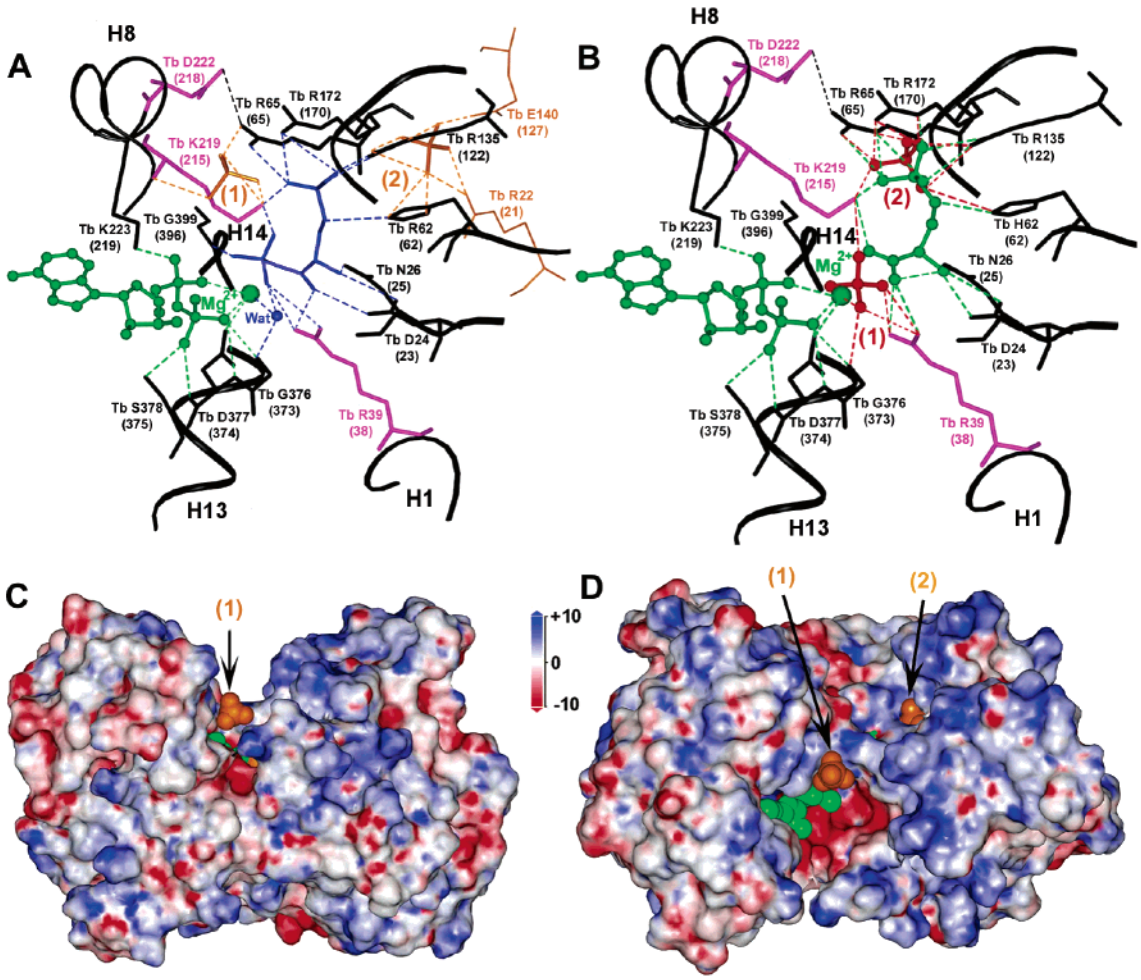

FIGURE 5: Interactions of the mutated side chains with substrates and anions in the active site of PGK. The surrounding helices (black ribbon) and the interacting side chains [black stick models, except for the highlighted (violet) Arg Tb39/38, Lys Tb219/215, and Asp Tb222/218] around the bound substrates (green) are shown as determined from the closed crystal structures of *T. brucei* (*67*) (A and B). The possible binding modes of 1,3-BPG (blue stick model) and modeled activating phosphate ions 1 and 2 (orange stick models), as determined by docking into the closed structure of *T. brucei* PGK ternary complex, are illustrated in panel A. The side chains interacting with only the modeled phosphates and not with the substrates are represented with orange sticks. In panel B, the red-colored phosphate ion 1 is bound in the crystal structure of the *T. brucei* PGK ternary complex with MgADP and 3-PG crystallized from phosphate (*67*), while the other red-colored phosphate ion 2 is determined in a separate structure of the pig muscle PGK binary complex with MgATP, crystallized from phosphate (*30*). The latter structure of pig muscle PGK (not shown) is superimposed with the structure of *T. brucei* PGK (shown here) according to the backbone atoms of their N-domain β-strands. The dashed lines represent H-bonds (up to 3.5 Å) and ionic interactions (up to 4.0 Å). In panels C and D, the surface-covered model of the closed structure of the *T. brucei* PGK molecule is shown, colored according to the calculated electrostatic potential map (red for positive, blue for negative, and white for neutral). Numbers indicate the binding sites of the modeled phosphates.

Stability and Conformation of the Mutant Proteins. Far- and near-UV CD spectra (not shown) showed no detectable conformational changes for all the investigated mutants of Lys 215 and Arg 38 compared to wild-type hPGK. This excludes the occurrence of gross conformational changes. The cooperative heat transition curves, as observed by DSC calorimetry (Figure 4A), also indicate the presence of well-folded structures for all mutants. The midtransition temperatures (T_m) do not deviate significantly (except that of R38A) from that of the wild-type enzyme. In the case of the R38A mutant, a decrease of as much as ~4−5 °C was observed in the T_m value. This is an indication of a more flexible structure of the mutant R38A, compared to the other mutants as well as to wild-type hPGK. This change correlates well with the smaller ΔH obtained in the case of R38A. In agreement, these thiol reactivity studies also indicate the occurrence of local conformational changes in the surrounding of the reactive thiol groups, since the number of fast-reacting thiols per protein molecule is largely increased with the R38A mutation, while it is not affected by the other mutations (Figure 4B). This conformational change upon mutation of Arg 38 was not detected in a previous NMR study where chemical shift perturbation of the histidine side chain at the 3-PG site was tested (*41*).

Docking of 1,3-BPG and of the Potential Activating Anion-(s) into Wild-Type PGK. Until now, there has been no direct crystallographic information about the mode of binding of 1,3-BPG to PGK. This substrate most probably binds to the same site where 3-PG binding is located. Accordingly, the binding mode of 1,3-BPG is suggested by Bernstein and Hol from their separate crystallographic data on 3-PG and phosphate ion binding (*67*). Binding studies using NMR chemical shift perturbation, carried out with various bisphosphonate analogues of 1,3-BPG (*68*−*70*), also approved its binding to the 3-PG site, but some uncertainty remained in its orientation in PGK active site. We modeled 1,3-BPG by

docking it into the active sites of the open conformation both of the binary complex of *Bacillus stearothermophilus* PGK with MgADP (*28*) (not shown) and of the closed conformation of the *T. brucei* PGK ternary complex with MgADP and 3-PG (*67*) (blue model in Figure 5A). In both cases, essentially similar binding modes of 1,3-BPG were obtained in place of 3-PG (cf. Figure 5B), showing good interaction of its 1-phosphate with the side chain of Arg 38/Bs36/Tb39, in agreement with the suggestion by Bernstein et al. (*67*). An additional interaction of the 1-phosphate of 1,3-BPG with Lys Tb219/215 in this closed structure is also supported by our modeling studies (Figure 5A), but no interaction with the equivalent Lys Bs197 of the docked 1,3-BPG could be detected in the open conformation of *B. stearothermophilus* PGK (not shown). It is to be noted that an O atom of the 1-phosphate of 1,3-BPG also forms a good H-bond with the main chain N atom of Gly Tb399/396 at the N-terminus of helix 14, not suggested previously (*67*). In the known crystal structure of the 3-PG binary complex of pig muscle PGK (*19*−*24*, *28*−*30*), the carboxylate group of 3-PG interacts loosely with the same Gly 396(N) atom, through a bound water molecule (Figure 1C). In the case presented here, an interaction through a water molecule is formed between the 1-phosphate of the modeled 1,3-BPG and the main chain N atom of Gly Tb376/373 at the N-terminus of helix 13, as well as with the catalytic Mg^{2+} (Figure 5A).

In searching for the possible activating site, we also modeled a phosphate ion into the closed ternary complex structure of *T. brucei* PGK, containing the modeled 1,3-BPG and the bound MgADP at the substrate binding sites. We found at least two different possibilities for binding of phosphate ion(s) as illustrated by orange models in Figure 5A. One modeled bound phosphate ion, numbered 1, binds through interactions with Arg Tb65/65 and Lys Tb219/215 in the interdomain region, but outside of the closed active site. This anion site is almost identical with the site obtained from previous modeling studies of our laboratory (*50*). Another phosphate ion, numbered 2, binds in a small, well-defined hole at the outer surface of the N-domain, with participation of 3-PG binding side chains His Tb62/62 and Arg Tb135/122, as well as with the conserved Arg Tb22/21, and also forms a H-bond with the carboxylate group of Glu Tb140/127. Among the interacting residues, mutagenesis studies provided reasonable arguments for only Arg 21 as a possible participant in the anion-dependent activation (*39*), but no clear results were obtained in the case of either His 62 (*39*, *41*) or Arg 122 (*24*−*26*, *38*−*43*). Binding of the modeled phosphates is also illustrated by the electrostatic surface map of the PGK molecule (Figure 5C,D). It may be notable that when the crystallographically bound water molecules were removed from the active site before docking, a third phosphate ion could be docked close to the 1-phosphate of the bound 1,3-BPG (not shown).

Docking of other anions (pyrophosphate, citrate, 3-PG, or 1,3-BPG) to the ternary MgADP−1,3-BPG complex has also resulted in binding to the anionic sites described above.

DISCUSSION

Lys 215 Is Essential for PGK Activity, while Asp 218 Is a Nonessential Residue. Here we demonstrate a drastic decrease in PGK activity (k_{cat} value) upon mutation of Lys 215, proving the essential role of this residue in the catalysis. Moreover, mutation to not only the neutral Ala (K215A) but also another positively charged residue, Arg (K215R), has led to an almost similar amount of activity lost (Table 1). The decrease in PGK activity with these mutations of Lys 215 cannot be due to improper folding of the structures, as evidenced by DSC, CD measurements, and thiol reactivity studies. At the same time, we show here that mutation of the known catalytic residue, Arg 38, to Ala (R38A) induces local conformational changes (Figure 4) that may contribute to the activity loss of this mutant. Furthermore, mutation of Arg 38 to Lys (R38K) only moderately perturbs the catalytic properties. Thus, in contrast to Arg 38, the size and shape of the side chain of Lys 215 are also essential for catalysis, besides its positive charge. This emphasizes the importance of the very precise positioning of Lys 215 in the enzyme active site.

In contrast to the drastic decrease in the k_{cat} values, a much smaller, but significant, decrease was obtained in the K_m values for the substrates, except MgADP, upon mutation of Lys 215. This further specifies the importance of Lys 215 during catalysis. The largest (20-fold) increase in the K_m of MgATP in the case of the neutral K215A mutant (relative to the absence of any change for MgADP) argues in favor of the role of Lys 215 in stabilization of the transferring γ-phospho group of the nucleotide. The significant (∼12-fold) increase in the K_m of 1,3-BPG, bearing the transferring 1-phosphate, is also consistent with this assumption. The moderate (∼3−4-fold) increase of the K_m value of 3-PG may be consistent with the X-ray pictures of the closed ternary complexes of *Th. maritima* (*22*) and of *T. brucei* PGK (*67*; Figure 5B) showing simultaneous interactions of Lys Tm197/Tb219/215 with both the 3-phosphate and the carboxylate of 3-PG.

With regard to the role of nearby Asp 218/Tb222, it is not an essential residue like Lys 215/Tb219, since PGK activity is decreased only 3-fold in the mutant D218N. Since neither the K_d nor the K_m values of MgATP are changed with this mutation, no evidence is provided in favor of the assumed ionic interaction of Asp 218 with Mg^{2+} (Figure 1B). The moderate (∼4-fold) increase in the K_m of 3-PG, however, may indicate that Asp 218 indirectly contributes to the interaction with 3-PG during catalysis. This may be achieved through the known salt bridge with Arg 65/Tb65/Tm62 as observed in the structures of *Th. maritima* (*22*) and of *T. brucei* (*67*) PGKs, i.e., with the residue that interacts with 3-PG (Figure 5A,B).

Mutation of Lys 215 Abolishes while Mutation of Asp 218 Reduces Substrate- and Anion-Dependent Activation: Location of the Activating Anion Site(s) by Modeling. Both mutations of Lys 215 abolish activation by either the excess substrates or anions, while mutation of Asp 218 to Asn largely suppresses both phenomena. As for other mutations, such as R38A [described previously (*39*, *41*) and confirmed here] as well as for R65A (*39*, *40*), the two activation phenomena are perturbed together. These findings support the previous suggestion (*50*) that the site for the activating anion and for the activating substrate is a common site. The location of this site is, however, still unknown, since neither NMR nor X-ray studies could identify an extra anionic site, independent of the catalytic substrate sites. Its detection by other physicochemical methods (e.g., using isothermal ti-

tration binding calorimetry) has also met with difficulty (A. Varga, B. Flachner, Z. Gugolya, F. Vonderviszt, and M. Vas, unpublished observations) that may be due to the extremely weak binding of the anions to this site. Despite these difficulties in proving the existence of the activating site, the observation that the essential catalytic residues, Arg 38 and Lys 215, are also essential for anion activation may indicate that the activating site is very close to the site of the transferring phosphate or that at a certain stage of the catalytic cycle the two sites are overlapping. This conclusion would also be compatible with the absence of activation in the enzyme reaction with 1,3 BPG, which is suggested from the results presented here. If, for example, 1,3-BPG possesses itself the activating phosphate, no further activation is required.

Previous (*50*) and present modeling studies of anion binding, indeed, showed the possibility of binding of additional anion(s) to the same basic residues that are already involved in substrate binding and catalysis (orange phosphate ions in Figure 5A,D).

Phosphate site 2 possibly exists independent of domain closure. The relevance of this site may be supported by the finding that mutation of one of its constituent residues, Arg Tb22/21, to Ala eliminates the anion-caused activation (*39*). Surveying the crystal structure around the modeled phosphate 2 suggests that this anion may weaken the interactions of the 3-phosphate of either 3-PG or 1,3-BPG with the enzyme. Further work is required to determine whether the function of this site is really activation or inhibition.

Phosphate ion 1 interacts with both Arg Tb65/65 and Lys Tb219/215. The side chain of Arg 65 was shown to be responsible for anion activation by mutagenesis studies (*30*), while the importance of Lys Tb219/215 in anion activation is proven by the work presented here. This site was also detected in the previous modeling by our laboratory (*50*). This bound anion may regulate domain closure and opening, for example, simply by simultaneously interacting with Arg 65 and Lys 215 in the closed conformation or by competing with Asp Tb222/218 in formation of the salt bridge with Arg Tb65/65 that fixes the closed conformation. The finding that the mutant D218N exhibits greatly diminished anion and substrate activation supports the latter assumption. Alternatively, anion binding may promote dissociation of the slowly dissociating product, 1,3-BPG, by competing in its interaction with Lys Tb219/215. In either way, binding of anion to phosphate site 1 can cause activation. The importance of anion activation is underlined by the fact that it is a widespread phenomenon among the enzymes that handle various anionic metabolites (*71*−*80*).

Modeling with other anions (pyrophosphate or citrate), in place of phosphate, has led to similar results. Furthermore, 3-PG or 1,3-BPG could also be docked to these, possibly activating anionic sites. Thus, the common molecular mechanism of the anion- and substrate-caused activation is further supported.

Existence of Two Cooperative Inhibiting Anionic Sites and Their Weakening upon Mutation. This kinetic study provided evidence for the existence of two cooperatively interacting inhibiting anionic sites. These sites are possibly equivalent with the two structurally determined phosphate sites (red models in Figure 5B) derived from two independent crystal structures. Site 1 has been identified in the X-ray structure of the closed conformation of the *T. brucei* PGK ternary complex with MgADP and 3-PG (*67*). This site seems to be identical with the 1-phosphate site of the bound 1,3-BPG, as suggested by Bernstein et al. (*67*). However, careful comparison of the positions of this crystallographically determined phosphate and the 1-phosphate of the modeled 1,3-BPG shows that, although they are close to each other, they are not overlapping. Thus, the cavity of the active site in the closed conformation is not fully packed, which may allow a certain level of mobility of the 1-phosphate of 1,3-BPG. This observation is consistent with the notion that binding of 1,3-BPG should not be as favorable as binding of the transition state. For the same reason, while the red phosphate site 1 is a putative inhibiting anion site, another anion can still bind very close to it. This latter anion can even fulfill an opposite, activating role, simply by promoting the dissociation of the tightly bound product, 1,3-BPG. Indeed, in addition to the two phosphates in Figure 5A, a third phosphate could also be modeled in this place, close to the 1-phosphate of the bound 1,3-BPG, when part of the crystallographically bound water molecules was removed from the active site before docking (not shown). The anion-assisted product dissociation seems to be a general activation mechanism in enzymology, and there are several examples in the literature (*71*−*74*).

The other putative inhibiting phosphate site 2 (Figure 5B) is identical with the 3-phosphate site of 3-PG as determined in the X-ray structure of the pig muscle PGK binary complex with MgATP, crystallized in the presence of phosphates, in which 3-PG does not occupy this site (*30*). This single anionic site of PGK already exists in the open structure, i.e., even in the substrate-free enzyme, as confirmed by earlier NMR studies and by our isothermal titration studies (A. Varga, B. Flachner, Z. Gugolya, F. Vonderviszt, and M. Vas, unpublished observations). This site is not influenced by the mutation of Lys Tb219/215, since this residue is far from the 3-phosphate site of 3-PG in the open PGK structure. Indeed, mutations of Lys 215 did not affect the binding constants of pyrophosphate (Table 1). This site 2 should be an inhibiting site, since binding of an anion here directly competes with either 3-PG or 1,3-BPG binding. While site 2 exists independent of the domain closure, anion site 1 may be characteristic of only the closed conformation.

Figure 5B shows that Lys Tb219/215 interacts with both phosphate ions. Mutations of Lys 215 in hPGK, indeed, cause slight weakening of the inhibition by pyrophosphate at one or both sites (we can only characterize them with a common K_I value) (Table 1).

Model of Substrate-Assisted Domain Closure: The Importance of Lys 215. The findings presented here provide a comprehensive picture of the essential role of Lys 215 in PGK catalysis. Since binding of MgATP, and not MgADP, is slightly weakened by mutations of Lys 215 (Table 1), it follows that the γ-phosphate of MgATP interacts weakly with the ϵ-amino group of Lys 215 already in the nonfunctioning open conformation of the enzyme. This supports the existence of an alternative binding site for MgATP phosphates at the N-terminus of helix 8 (Figure 1B) (*30*). This interaction may assist in the movement of helix 8 relative to helix 13 during domain closure and illustrated in Figure 1D. During this movement, the side chain of Lys 215 moves together with the γ-phosphate of MgATP at least ~10 Å (Figure 1A,D).

In addition, as follows from the kinetic results, in the closed conformation, the contact with Lys 215 is strengthened and this side chain stabilizes the transferring phospho group during the catalysis. This mechanism is an interesting example of a substrate-assisted movement of an essential catalytic residue.

Considering the reverse reaction, the question of whether the substrate 1,3-BPG could fulfill a similar role arises; i.e., would its 1-phosphate be able to initiate any interaction with Lys 215 already in the open enzyme conformation? Since no structural data are available, we have modeled binding of 1,3-BPG to the known open conformation of the MgADP binary complex, obtained from the crystal structure of *B. stearothermophilus* PGK (*28*). The more favorable binding mode of 1,3-BPG, however, does not show any interaction with Lys Bs197/215 but, instead, shows strong interaction with Arg Bs36/38. This finding is consistent with our binding data, showing no any change in the binding constant of 1,3-BPG upon mutation of Lys 215, but a rather drastic change upon mutation of Arg 38 to Ala (Table 1). Thus, in the reaction of 1,3-BPG with MgADP, no evidence in favor of operation of a substrate-assisted movement of the catalytic lysyl side chain is obtained. There are, however, other types of notions. Namely, (i) the 1-phosphate of the modeled bound 1,3-BPG, in addition to its interaction with Arg Tb39/38 at the N-terminus of helix 1, also interacts with Gly Tb399/396 at the N-terminus of helix 14, and (ii) the 1-phosphate of the bound 1,3-BPG is allowed to move to a certain extent, even within the closed active site cavity. On these bases, we propose that the 1-phosphate of the bound 1,3-BPG contributes to the movement of helix 14 closer to helix 1 during domain closure. The similar relative movement of these helices (~3 Å) indeed occurs also in the 3-PG binary complex of PGK (compared to the substrate-free enzyme, as illustrated in Figure 1C), leading to approximately the first 8° of domain rotation (*19*).

As a conclusion, mechanisms including substrate-assisted movements of interdomain helices may operate in both directions of the PGK-catalyzed reaction. Namely, at the initial phase of Michaelis complex formation, the transferring phosphate (i.e., in one direction the terminal phosphate of MgATP or in the other direction the 1-phosphate of 1,3 BPG) can interact with either the Lys 215 side chain of helix 8 or Gly 396(N) of helix 14, respectively. Thereby, in one direction, MgATP assists in an ~10 Å movement of helix 8 (bearing the catalytic residue Lys 215) toward the N-terminus of helix 13, while in the other direction, 1,3-BPG assists in an at least 3 Å movement of the N-termini of helix 14 toward helix 1 (bearing the catalytic residue Arg 38). These movements greatly contribute to the positioning of the two key important residues (Lys 215 and Arg 38), as well as of the N-termini of helices 13 and 14, to form the proper geometry of the active site for the phospho transfer.

ACKNOWLEDGMENT

Thanks are due to Prof. P. Hogg (Centre for Vascular Research, University of New South Wales) for providing us the plasmid of human PGK. We are indebted to Dr. P. Gál (Institute of Enzymology, BRC, Hungarian Academy of Sciences) for his valuable advise regarding protein expression work.

REFERENCES

1. Vishwanatha, J. K., Jindal, H. K., and Davis, R. G. (1992) The role of primer recognition proteins in DNA replication: Association with nuclear matrix in HeLa cells, *J. Cell Sci. 101*, 25−34.
2. Popanda, O., Fox, G., and Thielmann, H. W. (1998) Modulation of DNA polymerases α, δ and ϵ by lactate dehydrogenase and 3-phosphoglycerate kinase, *Biochim. Biophys. Acta 1397*, 102−17.
3. Ogino, T., Iwama, M., Kinouchi, J., Shibagaki, Y., Tsukamoto, T., and Mizumoto, K. (1999) Involvement of a cellular glycolytic enzyme, phosphoglycerate kinase, in Sendai virus transcription, *J. Biol. Chem. 274*, 35999−6008.
4. Xu, K. Y., Zweier, J. L., and Becker, L. C. (1995) Functional coupling between glycolysis and sarcoplasmic reticulum Ca^{2+} transport, *Circ. Res. 77*, 88−97.
5. Segel, G. B., Feig, S. A., Glader, B. E., Muller, A., Dutcher, P., and Nathan, D. G. (1975) Energy metabolism in human erythrocytes: The role of phosphoglycerate kinase in cation transport, *Blood 46*, 271−8.
6. Krishnan, P., Liou, J. Y., and Cheng, Y. C. (2002) Phosphorylation of pyrimidine L-deoxynucleoside analog diphosphates. Kinetics of phosphorylation and dephosphorylation of nucleoside analog diphosphates and triphosphates by 3-phosphoglycerate kinase, *J. Biol. Chem. 277*, 31593−600.
7. Krishnan, P., Fu, Q., Lam, W., Liou, J. Y., Dutschman, G., and Cheng, Y. C. (2002) Phosphorylation of pyrimidine deoxynucleoside analog diphosphates: Selective phosphorylation of L-nucleoside analog diphosphates by 3-phosphoglycerate kinase, *J. Biol. Chem. 277*, 5453−9.
8. Gallois-Montbrun, S., Faraj, A., Seclaman, E., Sommadossi, J. P., Deville-Bonne, D., and Veron, M. (2004) Broad specificity of human phosphoglycerate kinase for antiviral nucleoside analogs, *Biochem. Pharmacol. 68*, 1749−56.
9. Krishnan, P., Gullen, E. A., Lam, W., Dutschman, G. E., Grill, S. P., and Cheng, Y. C. (2003) Novel role of 3-phosphoglycerate kinase, a glycolytic enzyme, in the activation of L-nucleoside analogs, a new class of anticancer and antiviral agents, *J. Biol. Chem. 278*, 36726−32.
10. Lay, A. J., Jiang, X. M., Kisker, O., Flynn, E., Underwood, A., Condron, R., and Hogg, P. J. (2000) Phosphoglycerate kinase acts in tumour angiogenesis as a disulphide reductase, *Nature 408*, 869−73.
11. Hogg, P. J. (2003) Disulfide bonds as switches for protein function, *Trends Biochem. Sci. 28*, 210−4.
12. Lay, A. J., Jiang, X. M., Daly, E., Sun, L., and Hogg, P. J. (2002) Plasmin reduction by phosphoglycerate kinase is a thiol-independent process, *J. Biol. Chem. 277*, 9062−8.
13. Daly, E. B., Wind, T., Jiang, X. M., Sun, L., and Hogg, P. J. (2004) Secretion of phosphoglycerate kinase from tumour cells is controlled by oxygen-sensing hydroxylases, *Biochim. Biophys. Acta 1691*, 17−22.
14. Cao, R., Wu, H. L., Veitonmaki, N., Linden, P., Farnebo, J., Shi, G. Y., and Cao, Y. (1999) Suppression of angiogenesis and tumor growth by the inhibitor K1-5 generated by plasmin-mediated proteolysis, *Proc. Natl. Acad. Sci. U.S.A. 96*, 5728−33.
15. Stathakis, P., Fitzgerald, M., Matthias, L. J., Chesterman, C. N., and Hogg, P. J. (1997) Generation of Angiostatin by reduction and proteolysis of plasmin. Catalysis by a plasmin reductase secreted by cultured cells, *J. Biol. Chem. 272*, 20641−5.
16. Banks, R. D., Blake, C. C. F., Evans, P. R., Haser, R., Rice, D. W., Hardy, G. W., Merrett, M., and Phillips, A. W. (1979) Sequence, structure and activity of phosphoglycerate kinase: A possible hinge-bending enzyme, *Nature 279*, 773−7.
17. Mori, N., Singer-Sam, J., and Riggs, A. D. (1986) Evolutionary conservation of the substrate binding cleft of 3-phosphoglycerate kinases, *FEBS Lett. 204*, 313−7.
18. Watson, H. C., and Littlechild, J. A. (1990) Isoenzymes of phosphoglycerate kinase: Evolutionary conservation of the structure of this glycolytic enzyme, *Biochem. Soc. Trans. 18*, 187−90.
19. Harlos, K., Vas, M., and Blake, C. C. F. (1992) Crystal structure of the binary complex of pig muscle phosphoglycerate kinase and its substrate 3-phospho-D-glycerate, *Proteins 12*, 133−44.
20. May, A., Vas, M., Harlos, K., and Blake, C. C. F. (1996) 2.0 Å resolution structure of a ternary complex of pig muscle phosphoglycerate kinase containing 3-phospho-D-glycerate and the nucleotide Mn adenylylimidodiphosphate, *Proteins 24*, 292−303.

21. Bernstein, B. E., Michels, P. A. M., and Hol, W. G. J. (1997) Synergistic effects of substrate-induced conformational changes in phosphoglycerate kinase activation, *Nature 385*, 275−8.
22. Auerbach, G., Huber, R., Grättinger, M., Zaiss, K., Schurig, H., Jaenicke, R., and Jacob, U. (1997) Closed structure of phosphoglycerate kinase from *Thermotoga maritima* reveals the catalytic mechanism and determinants of thermal stability, *Structure 5*, 1475−83.
23. Szilágyi, A. N., Ghosh, M., Garman, E., and Vas, M. (2001) A 1.8 Å resolution structure of pig muscle 3-phosphoglycerate kinase with bound MgADP and 3-phosphoglycerate in open conformation: New insight into the role of the nucleotide in domain closure, *J. Mol. Biol. 306*, 499−511.
24. McPhillips, T. M., Hsu, B. T., Sherman, M. A., Mas, M. T., and Rees, D. C. (1996) Structure of the R65Q mutant of yeast 3-phosphoglycerate kinase complexed with Mg-AMP-PNP and 3-phospho-D-glycerate, *Biochemistry 35*, 4118−27.
25. Fairbrother, W. J., Walker, P. A., Minard, P., Littlechild, J. A., Watson, H., and Williams, R. J. P. (1989) NMR analysis of site-specific mutants of yeast phosphoglycerate kinase. An investigation of the triose-binding site, *Eur. J. Biochem. 183*, 57−67.
26. Fairbrother, W. J., Hall, L., Littlechild, J. A., Walker, P. A., Watson, H. C., and Williams, R. J. (1989) Site-directed mutagenesis of histidine 62 in the 'basic patch' region of yeast phosphoglycerate kinase, *FEBS Lett. 258*, 247−50.
27. Gregory, J. D., and Serpersu, E. H. (1993) Arrangement of substrates at the active site of yeast phosphoglycerate kinase. Effect of sulfate ion, *J. Biol. Chem. 268*, 3880−8.
28. Davies, G. J., Gamblin, S. J., Littlechild, J. A., Dauter, Z., Wilson, K. S., and Watson, H. C. (1994) Structure of the ADP complex of the 3-phosphoglycerate kinase from *Bacillus stearothermophilus* at 1.65 Å, *Acta Crystallogr. D50*, 202−9.
29. Kovári, Z., Flachner, B., Náray-Szabó, G., and Vas, M. (2002) Crystallographic and thiol-reactivity studies on the complex of pig muscle phosphoglycerate kinase with ATP analogues: Correlation between nucleotide binding mode and helix flexibility, *Biochemistry 41*, 8796−806.
30. Flachner, B., Kovári, Z., Varga, A., Gugolya, Z., Vonderviszt, F., Náray-Szabó, G., and Vas, M. (2004) Role of Phosphate Chain Mobility of MgATP in Completing the 3-Phosphoglycerate Kinase Catalytic Site: Binding, Kinetic, and Crystallographic Studies with ATP and MgATP, *Biochemistry 43*, 3436−49.
31. Fairbrother, W. J., Graham, H. C., and Williams, R. J. P. (1990) The roles of ATP^{4-} and Mg^{2+} in control steps of phosphoglycerate kinase, *Eur. J. Biochem. 190*, 407−14.
32. Graham, H. C., and Williams, R. J. P. (1991) The roles of ADP^{2-} and Mg^{2+} in control steps of phosphoglycerate kinase, *Eur. J. Biochem. 197*, 81−91.
33. Pappu, K. M., Kunnumal, B., and Serpersu, E. H. (1997) A new metal-binding site for yeast phosphoglycerate kinase as determined by the use of a metal-ATP analog, *Biophys. J. 72*, 928−35.
34. Raghunathan, V., Chau, M. H., Ray, B. D., and Rao, B. D. (1999) Structural characterization of manganese(II)-nucleotide complexes bound to yeast 3-phosphoglycerate kinase: ^{13}C relaxation measurements using [U-^{13}C]ATP and [U-^{13}C]ADP, *Biochemistry 38*, 15597−605.
35. Pickover, C. A., McKay, D. B., Engelman, D. M., and Steitz, T. A. (1979) Substrate binding closes the cleft between the domains of yeast phosphoglycerate kinase, *J. Biol. Chem. 254*, 11323−9.
36. Ptitsyn, O. B., Pavlov, M. Y., Sinev, M. A., and Timchenko, A. A. (1986) Study of domain displacements in proteins by diffuse X-ray scattering, in *Multidomain proteins* (Patthy, L., and Friedrich, P., Eds.) pp 9−25, Akadémiai Kiadó, Budapest.
37. Sinev, M. A., Razgulyaev, O. I., Vas, M., Timchenko, A. A., and Ptitsyn, O. B. (1989) Correlation between enzyme activity and hinge-bending domain displacement in 3-phosphoglycerate kinase, *Eur. J. Biochem. 180*, 61−6.
38. Barber, M. D., Gamblin, S. J., Watson, H., and Littlechild, J. A. (1993) Site-directed mutagenesis of yeast phosphoglycerate kinase. Arginines 65, 121 and 168, *FEBS Lett. 320*, 193−7.
39. Sherman, M. A., Szpikowska, B. K., Dean, S. A., Mathiowetz, A. M., McQueen, N. L., and Mas, M. T. (1990) Probing the role of arginines and histidines in the catalytic function and activation of yeast 3-phosphoglycerate kinase by site-directed mutagenesis, *J. Biol. Chem. 265*, 10659−65.
40. Sherman, M. A., Dean, S. A., Mathiowetz, A. M., and Mas, M. T. (1991) Site-directed mutations of arginine 65 at the periphery of the active site cleft of yeast 3-phosphoglycerate kinase enhance the catalytic activity and eliminate anion-dependent activation, *Protein Eng. 4*, 935−40.
41. Sherman, M. A., Fairbrother, W. J., and Mas, M. T. (1992) Characterization of the structure and properties of the His62→Ala and Arg38→Ala mutants of yeast phosphoglycerate kinase: An investigation of the catalytic and activatory sites by site-directed mutagenesis and NMR, *Protein Sci. 1*, 752−60.
42. Walker, P. A., Littlechild, J. A., Hall, L., and Watson, H. C. (1989) Site-directed mutagenesis of yeast phosphoglycerate kinase. The 'basic-patch' residue arginine 168, *Eur. J. Biochem. 183*, 49−55.
43. Walker, P. A., Joao, H. C., Littlechild, J. A., Williams, R. J., and Watson, H. C. (1992) Characterisation of yeast phosphoglycerate kinase modified by mutagenesis at residue 21, *Eur. J. Biochem. 207*, 29−37.
44. Fairbrother, W. J., Graham, H. C., and Williams, R. J. P. (1990) An NMR study of anion binding to yeast phosphoglycerate kinase, *Eur. J. Biochem. 190*, 161−9.
45. Scopes, R. K. (1978) Binding of substrates and other anions to yeast phosphoglycerate kinase, *Eur. J. Biochem. 91*, 119−29.
46. Wrobel, J. A., and Stinson, R. A. (1978) Anion binding to yeast phosphoglycerate kinase, *Eur. J. Biochem. 85*, 345−50.
47. Wrobel, J. A., and Stinson, R. A. (1981) The effects of anions, substrates, metal ions and sulfhydryl reagents on the proteolytic susceptibility of yeast phosphoglycerate kinase, *Biochim. Biophys. Acta 662*, 236−45.
48. Larsson-Raznikiewicz, M., and Schierbeck, B. (1977) The possibility that the substrates of phosphoglycerate kinase may specifically regulate the direction of its reversible reaction, *Biochim. Biophys. Acta 481*, 283−7.
49. Scopes, R. K. (1978) The steady-state kinetics of yeast phosphoglycerate kinase. Anomalous kinetic plots and the effects of salts on activity, *Eur. J. Biochem. 85*, 503−16.
50. Szilágyi, A. N., and Vas, M. (1998) Anion activation of 3-phosphoglycerate kinase requires domain closure, *Biochemistry 37*, 8551−63.
51. Larsson-Raznikiewicz, M. (1967) Kinetic studies on the reaction catalyzed by phosphoglycerate kinase. II. The kinetic relationships between 3-phosphoglycerate, $MgATP^{2-}$ and activating metal ion, *Biochim. Biophys. Acta 132*, 33−40.
52. Ali, M., and Brownstone, Y. S. (1976) A study of phosphoglycerate kinase in human erythrocytes. II. Kinetic properties, *Biochim. Biophys. Acta 445*, 89−103.
53. Burton, K. (1959) Formation constants for complexes of adenosine di- or tri-phosphate with magnesium or calcium ions, *Biochem. J. 71*, 388−95.
54. Larsson-Raznikiewicz, M. (1964) Kinetic studies on the reaction catalysed by phosphoglycerate kinase: I. The effect of Mg^{2+} and adenosine-5′-triphosphate, *Biochim. Biophys. Acta 85*, 60−8.
55. Gupta, R. K., Gupta, P., Yashok, W. P., and Rose, Z. B. (1983) Measurement of the dissociation constant of MgATP at physiological nucleotide levels by a combination of ^{31}P NMR and optical absorbance spectroscopy, *Biochem. Biophys. Res. Commun. 117*, 210−6.
56. Miller, C., Frey, C. M., and Stuehr, J. E. (1972) Interactions of divalent metal ions with inorganic and nucleotide phosphates. I. Thermodynamics, *J. Am. Chem. Soc. 94*, 8898−904.
57. Zhang, W., Truttmann, A. C., Luthi, D., and McGuigan, J. A. (1997) Apparent Mg^{2+}-adenosine 5-triphosphate dissociation constant measured with Mg^{2+} macroelectrodes under conditions pertinent to ^{31}P NMR ionized magnesium determinations, *Anal. Biochem. 251*, 246−50.
58. Negelein, E., and Brömel, H. (1939) *Biochem. Z. 301*, 135.
59. Furfine, C. S., and Velick, S. F. (1965) The Acyl-Enzyme Intermediate and the Kinetic Mechanism of the Glyceraldehyde 3-Phosphate Dehydrogenase Reaction, *J. Biol. Chem. 240*, 844−55.
60. Elödi, P., and Szörényi, E. (1956) Crystallisation and comparative studies of D-glyceraldehyde-3-phosphate dehydrogenase from muscle of various mammals, *Acta Physiol. Acad. Sci. Hung. 9*, 339−50.
61. Tompa, P., Hong, P. T., and Vas, M. (1986) The phosphate group of 3-phosphoglycerate accounts for conformational changes occurring on binding to 3-phosphoglycerate kinase. Enzyme inhibition and thiol reactivity studies, *Eur. J. Biochem. 154*, 643−9.
62. Cserpán, I., and Vas, M. (1983) Effects of substrates on the heat stability and on the reactivities of thiol groups of 3-phosphoglycerate kinase, *Eur. J. Biochem. 131*, 157−62.
63. Minard, P., Desmadril, M., Ballery, N., Perahia, D., Mouawad, L., Hall, L., and Yon, J. M. (1989) Study of the fast-reacting

cysteines in phosphoglycerate kinase using chemical modification and site-directed mutagenesis, *Eur. J. Biochem. 185*, 419−23.
64. Verdonk, M. L., Cole, J. C., Hartshorn, M. J., Murray, C. W., and Taylor, R. D. (2003) Improved protein−ligand docking using GOLD, *Proteins 52*, 609−23.
65. Lavoinne, A., Marchand, J. C., Chedeville, A., and Matray, F. (1983) Kinetic studies of the reaction mechanism of rat liver phosphoglycerate kinase in the direction of ADP utilization, *Biochimie 65*, 211−20.
66. Khamis, M. M., and Larsson-Raznikiewicz, M. (1981) Activation and inhibition of phosphoglycerate kinase by sulphate ion, *Biochim. Biophys. Acta 657*, 190−4.
67. Bernstein, B. E., and Hol, W. G. (1998) Crystal structures of substrates and products bound to the phosphoglycerate kinase active site reveal the catalytic mechanism, *Biochemistry 37*, 4429−36.
68. Caplan, N. A., Pogson, C. I., Hayes, D. J., and Blackburn, G. M. (1998) Novel bisphosphonate inhibitors of phosphoglycerate kinase, *Bioorg. Med. Chem. Lett. 8*, 515−20.
69. Jakeman, D. L., Ivory, A. J., Williamson, M. P., and Blackburn, G. M. (1998) Highly potent bisphosphonate ligands for phosphoglycerate kinase, *J. Med. Chem. 41*, 4439−52.
70. Jakeman, D. L., Ivory, A. J., Blackburn, G. M., and Williamson, M. P. (2003) Orientation of 1,3-bisphosphoglycerate analogs bound to phosphoglycerate kinase, *J. Biol. Chem. 278*, 10957−62.
71. Chegwidden, W. R., and Watts, D. C. (1984) Anion activation of monkey muscle creatine kinase, *Int. J. Biochem. 16*, 1171−4.
72. Harris, D. A., Dall-Larsen, T., and Klungsoyr, L. (1981) Studies of the kinetics of the isolated mitochondrial ATPase using dinitrophenol as a probe, *Biochim. Biophys. Acta 635*, 412−8.
73. Kasho, V. N., and Boyer, P. D. (1984) Relationships of inosine triphosphate and bicarbonate effects on F1 ATPase to the binding change mechanism, *J. Bioenerg. Biomembr. 16*, 407−19.
74. Roveri, O. A., and Calcaterra, N. B. (1985) Steady-state kinetics of F1-ATPase. Mechanism of anion activation, *FEBS Lett. 192*, 123−7.
75. Bunning, P., and Riordan, J. F. (1987) Sulfate potentiation of the chloride activation of angiotensin converting enzyme, *Biochemistry 26*, 3374−7.
76. Kramer, R., and Kurzinger, G. (1984) The reconstituted ADP/ATP carrier from mitochondria is both inhibited and activated by anions, *Biochim. Biophys. Acta 765*, 353−62.
77. Oikonomakos, N. G., Zographos, S. E., Tsitsanou, K. E., Johnson, L. N., and Acharya, K. R. (1996) Activator anion binding site in pyridoxal phosphorylase b: The binding of phosphite, phosphate, and fluorophosphate in the crystal, *Protein Sci. 5*, 2416−28.
78. Ravel, P., Craescu, C. T., Arous, N., Rosa, J., and Garel, M. C. (1997) Critical role of human bisphosphoglycerate mutase Cys22 in the phosphatase activator-binding site, *J. Biol. Chem. 272*, 14045−50.
79. Mizuguchi, H., Cook, P. F., Hasemann, C. A., and Uyeda, K. (1997) Chemical mechanism of the fructose-6-phosphate 2-kinase reaction from the pH dependence of kinetic parameters of site-directed mutants of active site basic residues, *Biochemistry 36*, 8775−84.
80. Contessi, S., Tanfani, F., Scire, A., Mavelli, I., and Lippe, G. (2001) Effects of Fe(III) binding to the nucleotide-independent site of F1-ATPase: Enzyme thermostability and response to activating anions, *FEBS Lett. 506*, 221−4.
81. Riddles, P. W., Blakeley, R. L., and Zerner, B. (1983) Reassessment of Ellman's reagent, *Methods Enzymol. 91*, 49−60.

BI051726G